

Power Quality Improvement & Energy Management Using Mmc Based Active Device

M.Ramesh¹

Assistant Professor¹, A.I.T.S-Rajampet, A.P, INDIA.

R. Madhan Mohan²

Assistant Professor², A.I.T.S-Rajampet, A.P, INDIA.

B. Ajeyudu³

PG Student³, A.I.T.S-Rajampet, A.P, INDIA.

Abstract

A transformer less hybrid series active filter is proposed to enhance the power quality in single-phase systems with critical loads. This paper assists the energy management and power quality issues related to electric transportation and focuses on improving electric vehicle load connection to the grid. The control strategy is de-signed to prevent current harmonic distortions of nonlinear loads to flow into the utility and corrects the power factor of this later. While protecting sensitive loads from voltage disturbances, sags, and swells initiated by the power sys- tem, rided of the series transformer, the configuration is advantageous for an industrial implementation. This polyvalent hybrid topology allowing the harmonic isolation and compensation of voltage distortions could absorb or inject the auxiliary power to the grid. Aside from practical analysis, this paper also investigates on the influence of gains and delays in the real-time controller stability. The simulations results are presented in this concept were carried out on a 2-kVA laboratory prototype demonstrating the effectiveness of the proposed topology.

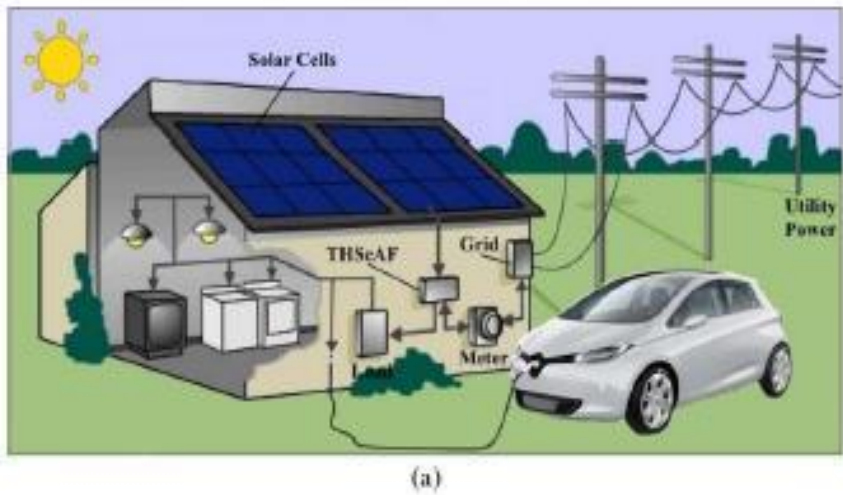
Keywords - Current harmonics, electric vehicle, hybrid series active filter (HSAF), power quality, and real-time control.

I. INTRODUCTION

The figure of future Smart Grids connected with electric vehicle charging stations has made a genuine worry on all parts of force nature of the force framework; while boundless electric vehicle battery charging units [1], [2] affect power dispersion framework consonant volt-age levels [3]. Then again, the development of sounds sustained from nonlinear burdens like electric vehicle drive battery chargers [4], [5], which surely impactfully affect the force framework and influence plant gear, ought to be considered in the improvement of cutting edge matrices. In like manner, the expanded rms and crest estimation of the twisted current waveforms build warming and misfortunes and cause the disappointment of the electrical gear. Such wonder adequately decreases framework proficiency and ought to have legitimately been tended to [6], [7].

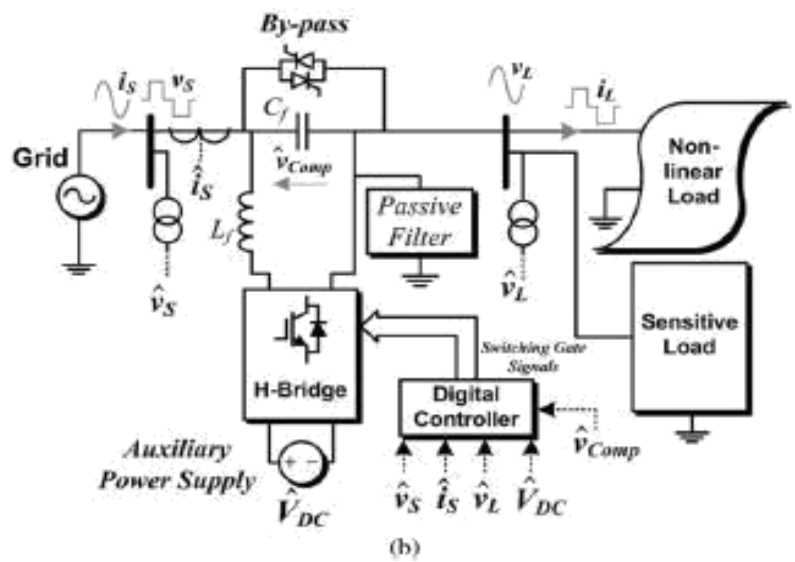
Additionally, to secure the purpose of regular coupling (PCC) from voltage mutilations, utilizing a dynamic voltage restorer (DVR) capacity is prompted. An answer is to lessen the contamination of force gadgets based loads straightforwardly at their source. They were created to dispose of current sounds delivered by nonlinear burden from the force framework. SeAFs are less scattered than the shunt sort of dynamic channels [8], [9]. The upside of the SeAF contrasted with the shunt sort is the second rate rating of the compensator versus the heap ostensible rating [10]. Be that as it may, the multifaceted nature of the setup and need of a disengagement arrangement transformer had decelerated their modern application in the dispersion framework. The second classification was created in worry of tending to voltage issues on touchy burdens. Normally known as DVR, they have a comparable setup as the SeAF. These two classes are not quite the same as each other in their control rule. This distinction depends on the reason for their application in the framework.

The benefit of the proposed arrangement is that non-straight Consonant voltage and current creating burdens could be viably adjusted. The transformerless mixture arrangement dynamic channel (THSeAF) is an option choice to routine force moving converters in circulated era frameworks with high entrance of renewable vitality sources, where every stage can be controlled independently and could be worked freely of different stages. This paper demonstrates that the detachment of a three-stage converter into single-stage H-span converters has permitted the end of the expensive disengagement transformer and advances modern application for sifting purposes. The setup has indicated extraordinary capacity to perform asked for remunerating errands for the revision of current and voltage contortions, PF amendment, and voltage reclamation on the heap terminal.



(a)

Fig.1: (a) Schematic of a single-phase smart load with the compensator installation



(b)

Fig.1: (b) Electrical diagram of the THSeAF in a single-phase utility.

This paper is sorted out as takes after. The framework design is presented in the accompanying segment. At that point, the operation rule of the proposed design is clarified. The third segment is committed to the demonstrating and investigation of the control calculation executed in this work. The dc voltage direction and its contemplations are quickly clarified, and the voltage and current symphonious recognition strategy is expressly portrayed.

To assess the setup and the control approach, a few situations are reenacted. Test results performed in the research facility are exhibited to approve recreations. This paper is condensed with a conclusion and supplement where further scientific improvements are illustrated.

II. SYSTEM ARCHITECTURE

A. System Configuration

The THSeAF appeared in Fig. 1 is made out of a H-span converter associated in arrangement between the source and the heap. A shunt inactive capacitor guarantees a low impedance way for current music. A dc assistant source could be associated with infuse power amid voltage lists. The dc-join vitality stockpiling framework is depicted in [19]. The framework is actualized for an appraised force of 2200 VA. To guarantee a quick transient reaction with adequate dependability edges over an extensive variety of operation, the controller is executed on a dSPACE/dsp1103.

The framework parameters are distinguished in Table I. A variable wellspring of 120 Vrms is associated with a 1.1kVA nonlinear burden and a 998-VA straight load with a 0.46 PF. The THSeAF is associated in arrangement to infuse the remunerating voltage. On the dc side of the compensator, a helper dc-join vitality stockpiling framework is introduced. Comparative parameters are likewise connected for functional usage.HSeAFs are often used to compensate distortions of the current type of nonlinear loads. For instance, the distorted current and voltage waveforms of the nonlinear system during normal operation and when the source voltage became distorted are depicted in Fig. 2. As one can perceive, even during normal operation, the current harmonics (with a total harmonic distortion (THD) of 12%) distort the PCC, resulting in a voltage THD of 3.2%.

TABLE I: CONFIGURATION PARAMETERS

Symbol	Definition	Value
v_s	Line phase-to-neutral voltage	120 Vrms
f	System frequency	60 Hz
$R_{non-linear\ load}$	Load resistance	11.5 Ω
$L_{non-linear\ load}$	Load inductance	20 mH
P_L	Linear load power	1 kVA
PF	Linear load power factor	46 %
L_f	Switching ripple filter inductance	5 mH
C_f	Switching ripple filter capacitance	2 μ F
T_s	dSPACE Synchronous sampling time	40 μ s
f_{PWM}	PWM frequency	5 kHz
G	Control gain for current harmonics	8 Ω
V_{DCref}^*	VSI DC bus voltage of the THSeAF	70 V
PI_G	Proportional gain (K_p), Integral gain (K_i)	0.025(4*), 10 (10*)

* Adopted value for the experimental setup

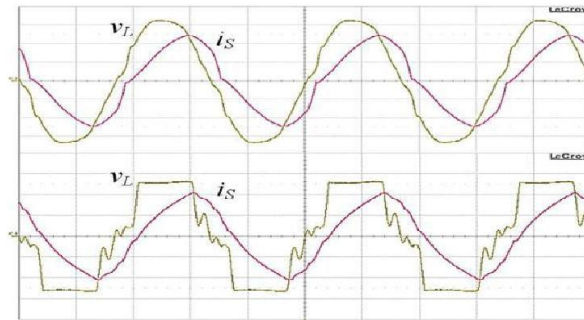


Fig.2: Terminal voltage and current waveforms of the 2-kVA single- phase system

without compensator. (a) Regular operation. (b) Grid’s voltage distortion (scales: 50 V/div for channel 1 and 10 A/div for channel 2).

The conduct of the framework when the matrix is profoundly contaminated with 19.2% of THD is likewise delineated. The proposed arrangement could be exclusively associated with the lattice with no need of a massive and expensive arrangement infusion transformer, making this topology equipped for remunerating source current music and voltage twisting at the PCC. Regardless of the possibility that the quantity of switches has expanded, the transformer less arrangement is more than whatever other arrangement compensators, which for the most part uses a transformer to infuse the remuneration voltage to the force framework. The enhanced uninvolved channel is made out of fifth, seventh, and high-pass channels. The latent channel ought to be balanced for the framework upon burden and government controls. An examination between various existing arrangements is given in Table II. It is planned to bring up the points of interest and disservices of the proposed arrangement over the customary topologies.

B. Operation Principle

The SeAF represents a controlled voltage source (VSI). In order to prevent current harmonics i_{Lh} to drift into the source, this series source should present low impedance for the fundamental component and high impedance for all harmonics as shown in Fig.3. The principle of such modeling is well documented.

The use of a well-tuned passive filter is then mandatory to perform the compensation of current issues and maintaining a constant voltage free of distortions at the load terminals. The behavior of the SeAF for a current control approach is evaluated from the phasor’s equivalent circuit shown in Fig.3. The nonlinear load could be modeled by a resistance representing the active power consumed and a current source generating current harmonics. Accordingly, the impedance Z_L represents the nonlinear load and the inductive load.

The SeAF operates as an ideal controlled voltage source (V_{comp}) having a gain (G) proportional to the current harmonics (I_{sh}) flowing to the grid (V_s)

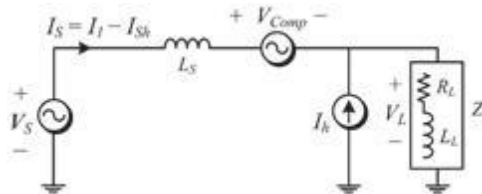


Fig.3: THSeAF equivalent circuit for current harmonics.

The SeAF operates as an ideal controlled voltagesource (V_{comp}) having a gain (G) proportional to the current harmonics (I_{sh}) flowing to the grid (V_s)

$$V_{comp} = G \cdot I_{sh} - V_{Lh} \quad (1)$$

This allows having individual equivalent circuit for the fundamental and harmonics

$$V_{source} = V_{s1} + V_{sh}, \quad V_L = V_{L1} + V_{Lh}. \quad (2)$$

The source harmonic current could be evaluated

$$V_{sh} = -Z_s \cdot I_{sh} + V_{comp} + V_{Lh} \quad (3)$$

$$V_{Lh} = Z_L (I_h - I_{sh}). \quad (4)$$

Combining (3) and (4) leads to (5)

$$I_{sh} = V_{sh} / (G - Z_s) \quad (5)$$

If gain G is sufficiently large ($G \rightarrow \infty$), the source current will become clean of any harmonics ($I_{sh} \rightarrow 0$). This will help improve the voltage distortion at the grid side. In this approach, the THSeAF behaves as high-impedance open circuit for current harmonics, while the shunt high-pass filter tuned at the system frequency creates a low-impedance path for all harmonics and open circuit for the fundamental; it also helps for PF correction.

III. MODELING AND CONTROL OF THE SINGLE-PHASE THSeAF

A. Average and Small-Signal Modeling

Based on the average equivalent circuit of an inverter [23], the small-signal model of the proposed configuration can be obtained as in Fig. 4. Hereafter, d is the duty cycle of the upper switch during a switching period, whereas v^- and i^- denote the average values in a switching period of the voltage and current of the same leg. The mean converter output voltage and current are expressed by (6) and (7) as follows:

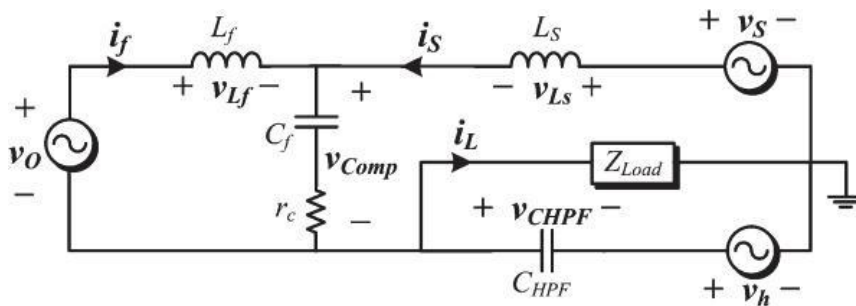


Fig.4: Small-signal model of transformer less HSeAF in series between the grid and the load.

$$V_o=(2d-1)V_{DC} \quad (6)$$

where the $(2d - 1)$ equals to m , then

$$I_{DC}=mif \quad (7)$$

Calculating the Thevenin equivalent circuit of the harmonic current source leads to the following assumption:

$$V_h= -jI_h/(CHPF.W_h) \quad (8)$$

If the harmonic frequency is high enough, it is possible to assume that there will be no voltage harmonics across the load. The state-space small-signal ac model could be derived by a linearized perturbation of the averaged model as follows:

$$\dot{x} = Ax + Bu \quad (9)$$

Moreover, the output vector is

$$y = Ax + Bu \quad (10)$$

By means of (9) and (10), the state-space representation of the model is obtained as shown in Fig. 4.

The transfer function of the compensating voltage versus the load voltage, $T_{V_CL}(s)$, and the source current, $T_{CI}(s)$, are developed in the Appendix. Meanwhile, to control the active part independently, the derived transfer function should be autonomous from the grid configuration. The transfer function T_{Vm} presents the relation between the output voltages of the converter versus the duty cycle of the first leg converter's upper switch

$$T_v(s) = \frac{V_{comp}}{V_o} = \frac{r_c C_f s + 1}{L_f C_f s^2 + r_c C_f s + 1} \quad (11)$$

$$T_{vm}(s) = \frac{V_{comp}}{m} = V_{DC} \cdot T_v(s) \quad (12)$$

The further detailed derivation of steady-state transfer functions is described in Section V.

A dc auxiliary source should be employed to maintain an adequate supply on the load terminals. During the sag or swell conditions, it should absorb or inject power to keep the voltage magnitude at the load terminals within a specified margin. Consequently, the dc-link voltage across the capacitor should be regulated as demonstrated in Fig. 5.

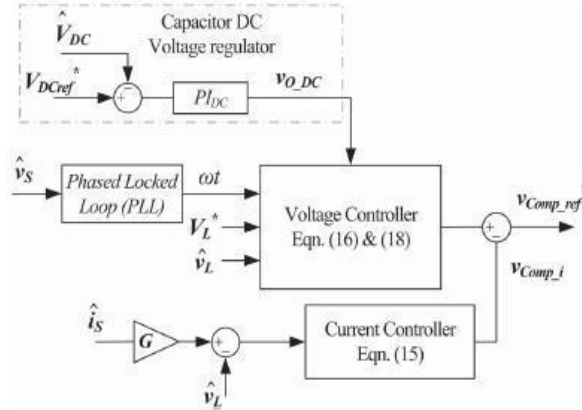


Fig.5: Control system scheme of the active part.

B. Voltage and Current Harmonic Detection

The outer-loop controller is used where a capacitor replaces the dc auxiliary source. This control strategy is well explained in the previous section. The inner-loop control strategy is based on an indirect control principle. A fast Fourier transformation was used to extract the magnitude of the fundamental and its phase degree from current harmonics.

The compensating voltage for current harmonic compensation is obtained from

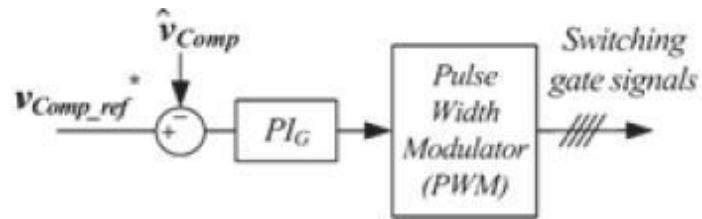


Fig.6: Block diagram of THSeAF and PI controller

Hereby, as voltage distortion at the load terminals is not desired, the voltage sag and swell should also be investigated in the inner loop. The closed-loop equation (16) allows to indirectly maintaining the voltage magnitude at the load side equal to V_L^* as a predefined value, within acceptable margins.

$$v_{comp_v} = \widehat{v}_L - V_L^* \sin(\omega_s t) \quad (13)$$

The entire control scheme for the THSeAF presented in Fig. 5 was used and implemented in MATLAB/Simulink for real-time simulations and the calculation of the compensating voltage.

$$v_{com_ref}^* = v_{comp-v} - v_{comp_i} + v_{DC_ref} \tag{14}$$

where the v_{DC_ref} is the voltage required to maintain the dc bus voltage constant

$$v_{DC_ref}(t) = V_{o_DC} \cdot \sin(\omega_s t) \tag{15}$$

A phase-locked loop was used to obtain the reference angular frequency (ω_s). Accordingly, the extracted current harmonic contains a fundamental component synchronized with the source voltage in order to correct the PF. This current represents the reactive power of the load. The gain G representing the resistance for harmonics converts current into a relative voltage. The generated reference voltage v_{comp_i} required to clean the source current from harmonics is described.

According to the presented detection algorithm, the compensated reference voltage v_{*Comp_ref} is calculated. Thereafter, the reference signal is compared with the measured output voltage and applied to a PI controller to generate the corresponding gate signals as in Fig. 6.

C. Stability Analysis for Voltage and Current Harmonics

The stability of the configuration is mainly affected by the introduced delay of a digital controller. This section studies the impact of the delay first on the inclusive compensated system according to works cited in the literature. The delay time of the digital controller, large gain G , and the high stiffness of the system seriously affect the stability of the closed-loop controlled system.

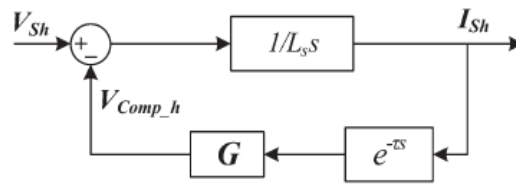


Fig.7: Control diagram of the system with delay.

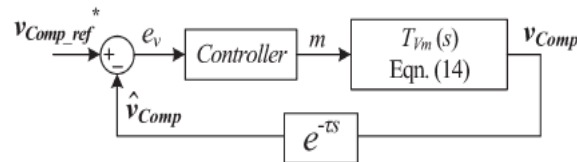


Fig.8: Closed-loop control diagram of the active filter with a constant delay time τ .

The compensating voltage including the delay time generated by the THSeAF in the Laplace domain [see (1)] is

$$v_{comp} = G \cdot I_{sh} \cdot e^{-\tau s} - V_{Lh} \quad (16)$$

Considering (19) and (20), the control diagram of the system with delay is obtained as in Fig. 7.

For the sake of simplicity, the overall delay of the system is assumed to be a constant value τ . Therefore, the open-loop transfer function is obtained

$$G(s) = \frac{G}{L_e s} e^{Ts} \quad (17)$$

From the Nyquist stability criterion, the stable operation of the system must satisfy the following condition:

$$G < \frac{\pi L_s}{2\tau} \quad (18)$$

A system with a typical source inductance L_s of 250

μH and a delay of $40 \mu\text{s}$ is considered stable according to (22) when the gain G is smaller than 10Ω . Experimental results confirm the stability of the system presented in this paper. Thus, assuming an ideal switching characteristic for the IGBTs, the closed-loop system for the active part controller is shown in Fig. 8.

A PI controller with system parameters described in Table I demonstrates a smooth operation in the stable region. By means of MATLAB, the behavior of the system's transfer function $F(s)$ is traced in Fig. 9. The root locus and the Bode diagram of the compensated open-loop system demonstrate a gain margin of 8.06 dB and a phase margin of 91° .

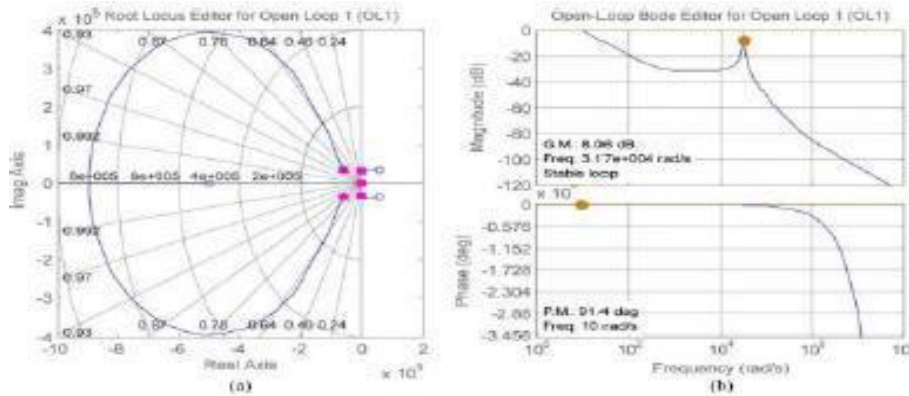


Fig.9: Compensated open-loop system with delay time of $40\mu\text{s}$.
(a) Root locus diagram. (b) Bode diagram.

IV. SIMULATIONS RESULTS

The proposed transformerless-HSeAF configuration was simulated in MATLAB/Simulink using discrete time steps of $T_s = 10 \mu s$. A dSPACE/dsp1103 was used for the fast control prototyping. To ensure an error-free and fast implementation, the complete control loop was executed every $40 \mu s$. The parameters are identified in Table I.

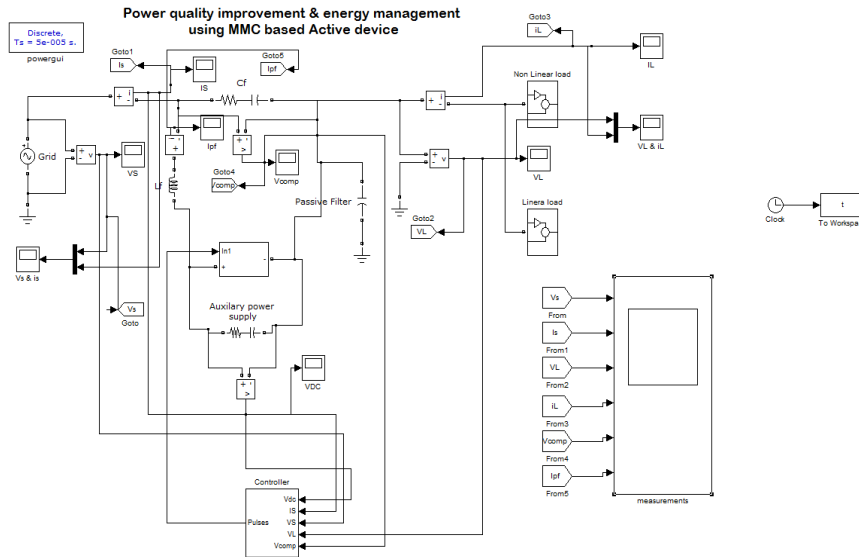


Fig.10: MATLAB simulated diagram

The combination of a single-phase nonlinear load and a linear load with a total rated power of 2 kVA with a 0.74 lagging PF is applied for simulations. For simulations, a 2-kVA 120-Vrms 60- Hz variable source is used. THSeAF connected in series to the system compensates the current harmonics and voltage distortions.

A gain $G = 8 \Omega$ equivalent to 1.9 p.u. was used to control current harmonics. As mentioned earlier, the capability of operation with low dc voltage is considered as one of the main advantages of the proposed configuration. For this simulation, it is maintained at 130 Vdc. During a grid's voltage distortion, the compensator regulates the load voltage magnitude, compensates current harmonics, and corrects the PF. The simulated results of the THSeAF illustrated in Fig. 11 demonstrates improvement in the source current THD.

The load terminal voltage VL THD is 4.3%, while the source voltage is highly distorted (THD VS = 25%). The grid is cleaned of current harmonics with a unity power factor (UPF) operation, and the THD is reduced to less than 1% in normal operation and less than 4% during grid perturbation. While the series controlled source cleans the current of harmonic components, the source current is forced to be in phase with the source voltage. The series compensator has the ability to slide the load voltage in order for the PF to reach unity. Furthermore, the series compensator

could control the power flow between two PCCs.

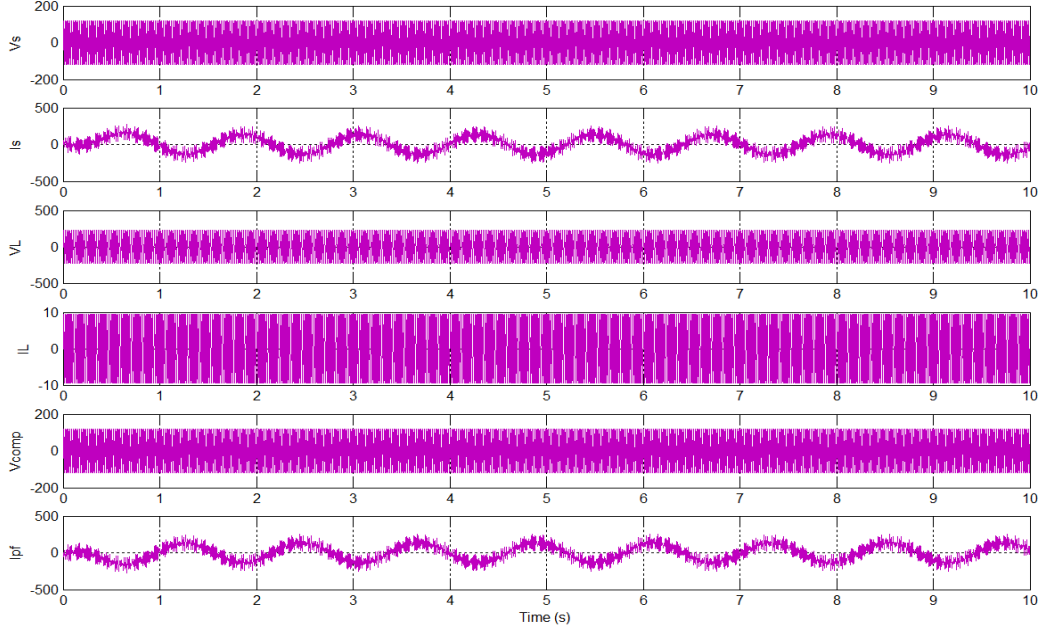


Fig.11: Simulation of the system with the THSeAF compensating current harmonics and voltage regulation. (a) Source voltage v_s , (b) source current i_s , (c) load voltage v_L , (d) load current i_L , (e) active-filter voltage V_{Comp} , and (f) harmonics current of the passive filter i_{PF} .

V. CONCLUSION

In this concept, a transformerless HSeAF for power quality improvement was developed by modular multilevel converter in MATLAB. The theory highlighted the fact that, with the ever increase of nonlinear loads and higher exigency of the consumer for a reliable supply, concrete actions should be taken into consideration for future smart grids in order to smoothly integrate electric car battery chargers to the grid. The key novelty of the proposed solution is that the proposed configuration could improve the power quality of the system in a more general way by compensating a wide range of harmonics current, even though it can be seen that the THSeAF regulates and improves the PCC voltage. Connected to a renewable auxiliary source, the topology is able to counteract actively to the power flow in the system. This essential capability is required to ensure a consistent supply for critical loads. Behaving as high-harmonic impedance, it cleans the power system and ensures a unity PF. The theoretical modeling of the proposed configuration was investigated. The proposed transformerless configuration was simulated. It was demonstrated that this active compensator responds properly to source voltage variations by providing a constant and distortion free supply at load terminals. Furthermore, it eliminates source harmonic currents and improves the power quality of the grid without the usual bulky and costly series transformer.

REFERENCES

- [1]. L. Jun-Young and C. Hyung-Jun, "6.6-kW onboard charger design using DCM PFC converter with harmonic modulation technique and two-stage dc/dc converter," *IEEE Trans. Ind. Electron.*, vol. 61, no. 3, pp. 1243–1252, Mar. 2014.
- [2]. R. Seung-Hee, K. Dong-Hee, K. Min-Jung, K. Jong-Soo, and L. Byoung-Kuk, "Adjustable frequency duty-cycle hybrid control strategy for full-bridge series resonant converters in electric vehicle chargers," *IEEE Trans. Ind. Electron.*, vol. 61, no. 10, pp. 5354–5362, Oct. 2014.
- [3]. P. T. Staats, W. M. Grady, A. Arapostathis, and R. S. Thallam, "A statistical analysis of the effect of electric vehicle battery charging on distribution system harmonic voltages," *IEEE Trans. Power Del.*, vol. 13, no. 2, pp. 640–646, Apr. 1998.
- [4]. A. Kuperman, U. Levy, J. Goren, A. Zafransky, and A. Savernin, "Battery charger for electric vehicle traction battery switch station," *IEEE Trans. Ind. Electron.*, vol. 60, no. 12, pp. 5391–5399, Dec. 2013.
- [5]. Z. Amjadi and S. S. Williamson, "Modeling, simulation, control of an advanced Luo converter for plug-in hybrid electric vehicle energy-storage system," *IEEE Trans. Veh. Technol.*, vol. 60, no. 1, pp. 64–75, Jan. 2011.
- [6]. H. Akagi and K. Isozaki, "A hybrid active filter for a three-phase 12-pulse diode rectifier used as the front end of a medium-voltage motor drive," *IEEE Trans. Power Del.*, vol. 27, no. 1, pp. 69–77, Jan. 2012.
- [7]. A. F. Zobaa, "Optimal multiobjective design of hybrid active power filters considering a distorted environment," *IEEE Trans. Ind. Electron.*, vol. 61, no. 1, pp. 107–114, Jan. 2014.
- [8]. D. Sixing, L. Jinjun, and L. Jiliang, "Hybrid cascaded H-bridge converter for harmonic current compensation," *IEEE Trans. Power Electron.*, vol. 28, no. 5, pp. 2170–2179, May 2013.
- [9]. M. S. Hamad, M. I. Masoud, and B. W. Williams, "Medium-voltage 12-pulse converter: Output voltage harmonic compensation using a series APF," *IEEE Trans. Ind. Electron.*, vol. 61, no. 1, pp. 43–52, Jan. 2014.
- [10]. J. Liu, S. Dai, Q. Chen, and K. Tao, "Modelling and industrial application of series hybrid active power filter," *IET Power Electron.*, vol. 6, no. 8, pp. 1707–1714, Sep. 2013.
- [11]. A. Javadi, H. Fortin Blanchette, and K. Al-Haddad, "An advanced control algorithm for series hybrid active filter adopting UPQC behavior," in *Proc. 38th Annu. IEEE IECON*, Montreal, QC, Canada, 2012, pp. 5318–5323.
- [12]. O. S. Senturk and A. M. Hava, "Performance enhancement of the single-phase series active filter by employing the load voltage waveform reconstruction and line current sampling delay reduction methods,"

